SAE TECHNICAL PAPER SERIES

982616

End Gas Inhomogeneity, Autoignition and Knock

J. Pan, C. G. W. Sheppard and A. Tindall
School of Mechanical Engineering, The University of Leeds

M. Berzins, S. V. Pennington and J. M. Ware
School of Computer Studies, The University of Leeds

SAE The Engineering Society For Advancing Mobility Land Sea Air and Space®
INTERNATIONAL

International Fall Fuels and Lubricants Meeting and Exposition
San Francisco, California
October 19-22, 1998

400 Commonwealth Drive, Warrendale, PA 15096-0001 U.S.A. Tel: (724) 776-4841 Fax: (724) 776-5760

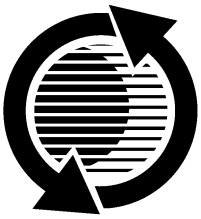

ISSN 0148-7191

Printed in USA

982616

End Gas Inhomogeneity, Autoignition and Knock

J. Pan, C. G. W. Sheppard and A. Tindall
School of Mechanical Engineering, The University of Leeds

M. Berzins, S. V. Pennington and J. M. Ware
School of Computer Studies, The University of Leeds

ABSTRACT

An advanced gas dynamic/chemistry interaction code, SPRINT2D, has been developed to simulate end gas autoignition and knock. This confirms that an earlier hypothesis of three distinct modes of autoignition was not an artefact of the previous numerical code. A comprehensive chemical kinetic scheme has predicted autoignition onset and demonstrated a mechanism for creating the end gas temperature gradients assumed in, as well as generated heat release rates for use in, SPRINT2D.

Using the combined modelling techniques, good matches between theoretical and experimental autoignition centre growth (at up to 750,000 frames/second), particle tracking and pressure development sequence at multiple transducer sites have been obtained for “thermal explosion” and “developing detonation” autoignition events.

INTRODUCTION

The onset of “knock” (or pinking), characterised by in-cylinder pressure oscillation and noise generation, ultimately limits spark ignition engine compression ratio and so thermal efficiency and potential for CO_2 emission reduction. It is generally accepted [1-4] that knock is triggered by end gas autoignition, sometimes termed “post-ignition” in order to distinguish the phenomenon from “pre-ignition” [5]. Hence knock can be avoided if the transit time for the spark ignited turbulent flame front is kept shorter than the (ignition delay) time required for the end gas spontaneously to ignite. Advances in “thermodynamic” and “multidimensional” engine cycle modelling codes allow the combustion duration to be predicted with a reasonable degree of accuracy. Similarly, fairly mature chemical reaction schemes now exist (at least for primary reference fuels) for estimating the time required for autoigntion to develop in response to temperature increase induced by chemical reaction and the combined compressive effects of piston motion and expansion of the burned gas consumed by the advancing (spark ignited) main flame. Hence it should be possible to predict (and so avoid) autoignition and subsequent knock. Equally, modern engine management systems are able to detect knock in individual cylinders and rapidly retard ignition timing for the appropriate cylinder in order to prevent knock. Herein lies a paradox, for in seeking to optimise efficiency such systems inevitably maintain each engine cylinder close to the threshold of knock under certain engine operating conditions. Because of the nature of cyclic variation in engines, post ignition will inevitably occur in a proportion of cycles. It has been observed that such autoignition can occur without inducing knock [1]; where this pertains, it may actually be beneficial in raising thermal efficiency and “cleaning up” unburned hydrocarbons by accelerating the slow final stages of combustion. It has been suggested [3,6] that where post-ignition occurs, it may develop in one of three modes (or some combination of these). These modes result from inhomogeneity in the end gases, previously characterised in terms of a temperature gradient about the “autoignition centre” where reaction first proceeds (in practice, compositional inhomogeneity may have a similar effect). With decreasing magnitude of temperature gradient, these three modes have been dubbed “deflagration”, “developing detonation” and “thermal explosion”. Temperature gradients in the unburned charge are inevitable – resulting from imperfect mixing of fuel, air and residual gases, non-homogenous turbulence, as well as heat transfer with walls (piston, valves, cylinder head, spark plug - each at different temperatures). The new generation of gasoline direct injection (GDI) engines is actually designed to promote charge inhomogeneity. Within the end gas, chemical reaction proceeding at different rates appropriate to the local temperature will accentuate any initial temperature variation.

The deflagrative mode, producing little or no knock, may (as outlined above) actually be beneficial. The explosive autoignition occurring with a homogenous end gas can produce severe knock intensity (pressure oscillations and objectional noise) but, arguably, may not result in

wall loading intense enough to produce physical damage to the engine [1] except possibly by general overheating of its components [7]. However, the developing detonation mode (with strong coupling between gas dynamics and chemical reaction) is likely to result in physically damaging transient, localised, extreme pressure and temperature excursions. This can possibly occur at lower "knock intensities" (expressed in terms of common indices [8] than for some thermal explosion-like events. The strong pressure waves associated with developing detonation may be sufficient to promote similarly destructive reaction in crevices [9]. Unfortunately, interaction between adjacent (benign) deflagrative autoignition events may lead to modified temperature gradients conducive to later transition to the (destructive) developing detonation mode [3]. Given the coupled nature of the developing detonation mode, it is perhaps unsurprising that it should be dependent upon the chemical heat release rate as well as the inhomogeneity [10], possibly explaining the "quieter knocking" noted with some fuel blends [11].

Earlier theoretical investigation of these phenomena employed the Leeds University Modes of Autoignition Development (LUMAD) code. However, confidence in quantitative predictions by LUMAD for actual experimental cycles was limited by its use of castellated cartesian co-ordinates (leading to accumulation of errors associated with spurious wall reflection of pressure waves) and, possibly, inadequate computation of events in regions of very steep pressure gradients. In the currently reported study a more advanced numerical code, SPRINT2D was used [12]. This employed triangular grids, spatial and temporal adaptivity, with high accuracy finite volume schemes to eliminate oscillations on shocks/fronts [13] to avoid the shortcomings of LUMAD. The new code was first applied to an idealised test case and an experimental cycle reported previously [3], in order to assess grid sensitivity and permit comparison with LUMAD solutions. Then the validity of the simple one step Arrhenius expression adopted in the code's energy equation source term was checked against the heat release rate output by a comprehensive chemical kinetic code [14]. This was then incorporated into the SPRINT2D code, in the form of a polynomial relation between rate of heat release and temperature. Finally, predictions of autoigntion development were compared with experimental data in the form of ultra high-speed (240,000 – 720,000fps) schlieren images generated at Daimler Benz [15], and analysed in Leeds [16].

THEORETICAL MODELLING

The end gas events of particular interest are those associated with the exceedingly fast 'thermal explosion' and 'developing detonation' autoignition modes. The 'propagation speeds' for the 'leading edges' (e.g. as seen in schlieren images) of such reactions are orders of magnitude faster than laminar and turbulent burning velocities. They result from 'distributed' chemical reaction or chemical reaction at shocks, rather than normal flame propagation. Hence, as described below and in common with the earlier LUMAD program [6], SPRINT2D is essentially a gas dynamic/chemical reaction code. In solving the mass, momentum and energy conservation equations, it does not invoke the turbulent diffusion or flame propagation (e.g. flamelet) terms of usual combustion CFD formulations. It could be argued that such terms need inclusion correctly to represent slower 'deflagrative' autoignition events. As described below, in the current work, computing effort has been concentrated in representing properly the more violent developing detonation mode of autoignition.

SPRINT2D SOFTWARE - The SPRINT2D software [13] solves time-dependent partial differential equations by using the method of lines to discretise in space, thus reducing the partial differential equations, PDEs, to a system of ordinary differential equations, ODEs, which can then be integrated using existing software packages. The code uses a cell-centred finite volume method in which the PDE is integrated over an element and the divergence theorem applied to replace the area integral for the fluxes by a line integral around the edge of the element. The flux functions in the PDE are then used to calculate the numerical flux between adjoining elements. Although the finite volume method may use any form of spatial elements, the use of triangular elements allows complex domains to be modelled and (when used in conjunction with temporal local error control and spatial error estimation and control) provides a powerful and reliable solver.

The form of the PDEs solved by SPRINT2D appropriate to this work was:

$$\beta \frac{\partial \underline{U}}{\partial t} + \frac{\partial}{\partial x} \underline{f}^x + \frac{\partial}{\partial y} \underline{f}^y = \underline{S} \qquad (1)$$

The driving program for SPRINT2D specifies the PDEs and the solution techniques to be used. The user, in this application, was required to specify the following information: a file containing a specification of the physical domain; relative and absolute tolerances for the adaptivity routines; a Riemann solver for the advective fluxes $\underline{f}^x$, $\underline{f}^y$ and a source term function $\underline{S}$; boundary and initial conditions.

Mathematically the problem was specified by a system of five PDEs representing conservation of mass, momentum and energy together with a species equation. The functions in Eq. 1 were defined by:

$$\underline{U} = (\rho,\ \rho u,\ \rho v,\ E,\ \rho z)^T \qquad (2)$$

and,

$$\underline{f}^x = \begin{pmatrix} \rho u \\ \rho u^2 + p \\ \rho uv \\ u[E + p] \\ \rho uz \end{pmatrix}, \quad \underline{f}^y = \begin{pmatrix} \rho v \\ \rho uv \\ \rho v^2 + p \\ v[E + p] \\ \rho uz \end{pmatrix}, \quad \underline{S} = \begin{pmatrix} 0 \\ 0 \\ 0 \\ 0 \\ -\rho z\, k(T) \end{pmatrix} \tag{3}$$

The variables ρ, *u, v, p* denote the density, velocities in x and y directions and pressure respectively. The variable *z* represents the unburned fuel mass fraction. The energy per unit volume, *E*, was defined by [6]:

$$E = \frac{p}{(\gamma - 1)} + \frac{\rho u^2 + \rho v^2}{2} + \alpha \rho z \tag{4}$$

and,

$$k(T) = exp\left[\beta\left(1 - \frac{1}{T}\right)\right] \tag{5}$$

governed the rate of reaction of fuel via a single step Arrhenius reaction. All parameters were normalised as outlined in Ref. [6]. As before the values of normalised heat release rate per unit mass of fuel (α) and normalised activation energy (β) were initially taken as 8 and 20 respectively, for assumed initial autoignition (centre) temperature close to 1000K, as suggested by Zel'dovitch et al [17]. Later, the Arrhenius expression was substituted by an empirical expression fitted to the heat release rate governed by a chemical kinetic model. The value of γ was set at 1.2 throughout.

MESH GENERATION AND ADAPTIVITY - the main attraction of unstructured triangular meshes was that they could approximate arbitrary domains more easily than quadrilateral based meshes. The initial meshes used in SPRINT2D were created from a geometry description using the GEOMPACK [18] mesh generator. This constructed the mesh by decomposing the input geometry into simpler polygons and then meshing these polygons. These meshes were then refined and coarsened by the TRIAD adaptivity module. The approach was to refine uniformly each triangle into four sub-triangles, thus defining a mesh at the next level up. Hence a Level 1 mesh had four times as many elements as the coarse mesh, a Level 2 mesh had 16 times as many elements and so on.

Full details of the computational methods, including particulars of the adaptive grid refinement (and de-refinement) as well as temporal and spatial error control procedures, are available elsewhere [19].

IDEALISED TEST CASE - The SPRINT2D code was first applied to an idealised test problem previously modelled using the earlier LUMAD program [3]. The geometry is set out in Fig. 1. The main flame front was represented by an arc of a circle of radius 0.7D, with D the cylinder diameter. A stoichiometric iso-octane mixture was assumed with the unburned and burned gases ahead of and behind this front at 500K and 2300K respectively; the two symmetrically located autoignition centres were assumed to be at 1000K initially. Computations were made for a range of (linear) temperature gradients (g) about the autoignition centres; the "actual" gradient being numerically equal to 12.5g K/mm. The numbered points around the circumference in Fig. 1 represent pressure transducer "locations". The computations were for a fixed "Level 5" grid (8192 elements).

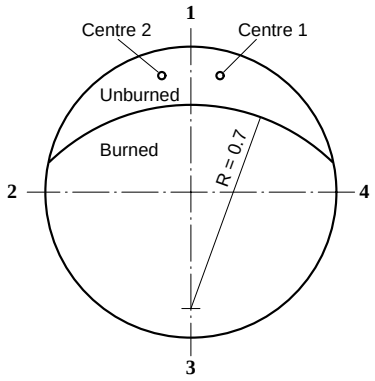

Fig. 1 Idealised test case geometry (burned gas region at 2300K, unburned gas at 500K, centres at 1000K)

Large temperature gradient (g = -10, -125K/mm) - It can be seen in Fig. 2 that the pressure at "transducer" Site 1, that closest to the autoignition centres, rises relatively late (~20μs) and gradually increases to a modest level (approximately 1.3 times the initial pressure (P_o)). The pressure rises (slightly) rather later at Sites 2 and 4 (~70μs) and later still at Site 4 (~90μs). This case has the features of a deflagration [3,6].

Small temperature gradient (g = -0.1, -1.25K/mm) - With such a small temperature gradient one might expect almost simultaneous reaction throughout the end gas region (i.e. a thermal explosion). A pressure rise was registered, at Site 1, after about 8μs. The pressure rise was abrupt, to quite a high level (~2.5P_o). Strong pressure rises were registered at Sites 2 and 4 after ~20μs and at the wall opposite the end gas region (Site 3) at about 60μs. The pressure registered here was ~3.5P_o (about 175bar). Nevertheless, this pressure was well below the 350bar figure estimated to be needed to cause physical damage to a piston [8].

Intermediate temperature gradient (g = -1.0, -12.5K/mm; g = -4.0, -60K/mm) - For g = -1, the earlier LUMAD code suggested that the autoignition would transform into a

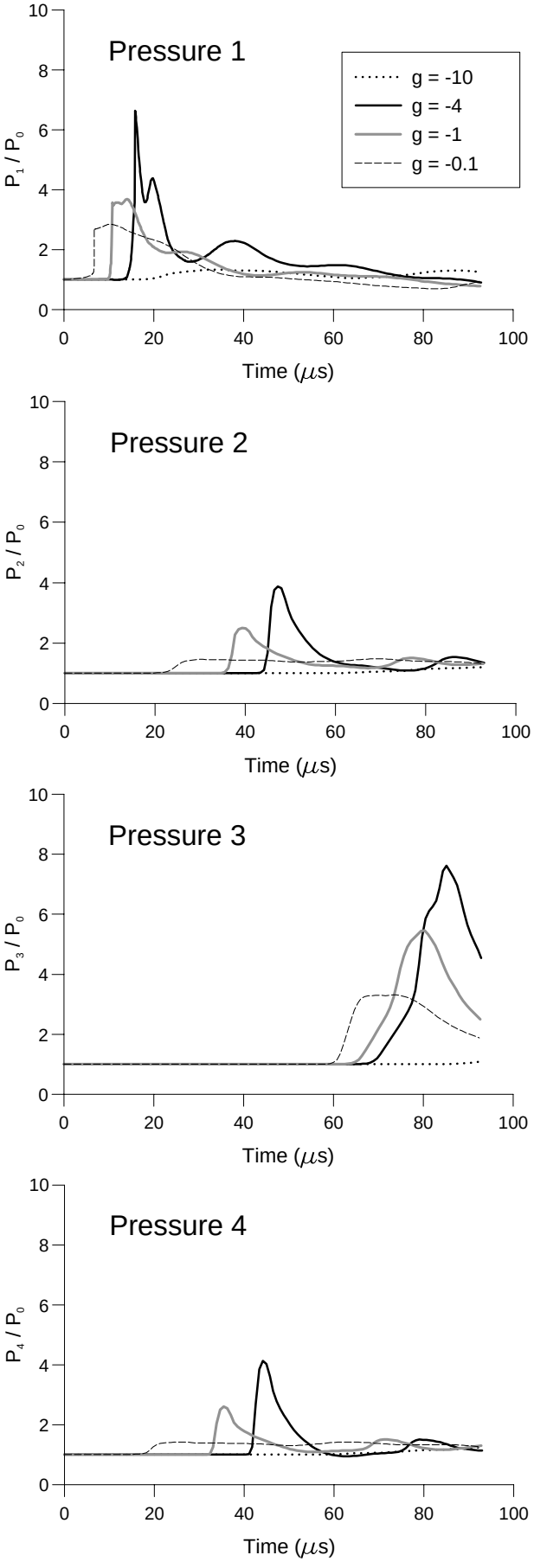

Fig. 2 Modelled pressure-time histories (idealised test case for a range of linear temperature gradients)

developing detonation [3]. The SPRINT2D program output implied a less violent event. The pressure rise at Site 1, Fig. 2, occurred later and to a higher level than noted in the small temperature gradient case – it also had a stronger rarefaction. A strong pressure rise (to $2.5P_o$) at Sites 2 and 4 was predicted at about 35μs. Unlike the small temperature gradient case, the pressure rise here proved transient. A strong wave reached Site 3 at about 80μs, with a transient pressure of ~$5P_o$ predicted. These features suggest the emergence of a "developing detonation". With a gradient of –4, the strong pressure spikes characteristic of a developing detonation were more marked; with transient overpressures as high as $8P_o$ registered.

In comparison with the earlier LUMAD results for this same test case [3], with SPRINT2D's better numerical procedures, computed pressure development was generally faster and to lower levels. Nevertheless, the three autoignition modes were again clearly demonstrated. For the developing detonation mode, similar extreme transient overpressures (sufficient to cause material damage) were noted; albeit at higher values of temperature gradient. The pressure "records" generally exhibited less spurious secondary "wiggles" than those with LUMAD, presumably associated with better physical representation of the cylinder boundaries and improved numerical procedures.

MODEL APPLICATION A

The SPRINT2D code was next applied to a moderate knock experimental cycle, principally to explore the effect of grid refinement and adaptivity. Since the experimental results have been presented previously [3] only an abbreviated description of them is presented here.

EXPERIMENT - The engine used was a heavily modified JLO 2-stroke engine of 80mm bore and 74mm stroke. The combustion space was a cylindrical disc formed by the barrel, a flat topped piston (fitted with a surface mirror in schlieren experiments) and a quartz top window allowing overhead optical access to the complete combustion space. The exhaust port was extended vertically upward such that the clearance height at TDC was reduced to 2.8mm, with a compression ratio of 10, to give an essentially 2-D combustion chamber for improved schlieren images and better compliance with the modelling assumptions. Side ignition was adopted and the cylinder head was fitted with 4 flush fitting Kistler 603B pressure transducers (of natural frequency ~400kHz) symmetrically placed around the chamber circumference. A further barrel fitted absolute pressure transducer was used to provide a reference pressure early in the cycle. The engine was operated in skip fire mode (generally with 4 skip cycles) on a stoichiometric mixture of a primary reference fuel of 90% iso-octane/10% n-heptane and air. A system for seeding the in-cylinder mixture with carbonaceous particles was also available. These particles burned behind the main flame

front and provided a means of tracking post-autoignition gas motion for comparison with model output. Fuller details of this system, as well as the filming, data acquisition and processing methods are set out in an earlier paper [3] and elsewhere [16, 20].

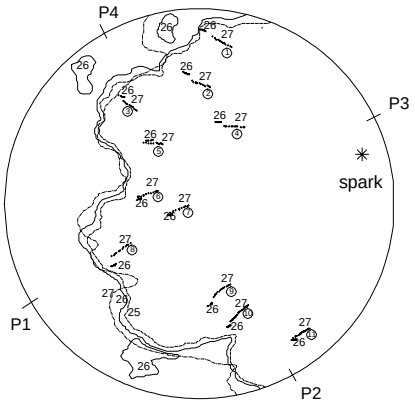

Time between two successive frames:
0.124 ms (1.1 deg CA)

Exposure time for a frame:
0.025 ms

Derived particle velocity (m/s) during the exposure time:

Frame	26	27
Particle 1:	31	176
Particle 2:	54	155
Particle 3:	42	132
Particle 4:	60	167
Particle 5:	49	156
Particle 6:	32	157
Particle 7:	31	159
Particle 8:	47	188
Particle 9:	36	178
Particle 10:	34	202
Particle 11:	30	148
CA (aTDC):	4.0	5.1

(a). Particle tracks during autoignition

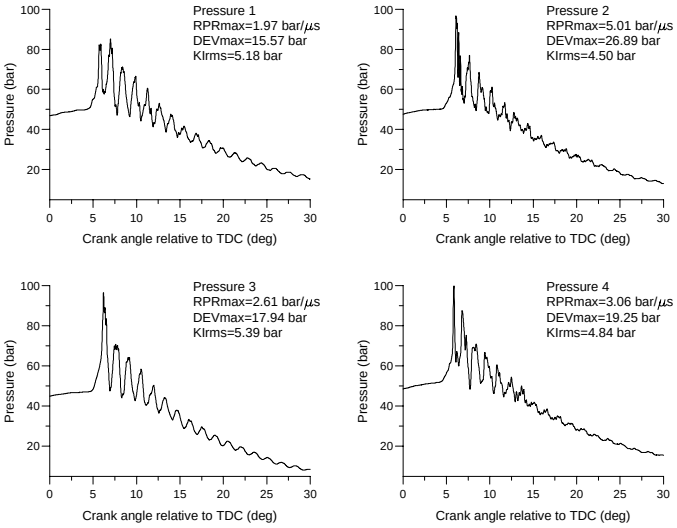

(b). Pressure records simultaneously measured at four different positions

Fig. 3 Experimental data for a moderate knock cycle (engine speed 1500 rpm, camera speed ~8000 fps)

Shown in Fig. 3, reproduced from Ref.[3] are diagrams showing particle tracks and tracings of main flame and end gas autoignition development derived from successive natural light ciné images recorded at 8065fps using a Hitachi 16mm camera; the engine speed was 1503rpm. Also shown are calculated particle velocities, pressure records at the 4 positions indicated and derived "knock intensity" parameters [21, 22]. These include a KIrms, expressing the root mean square deviation of pressure measured over a period of 2ms after being triggered by a pressure rise of 0.5 bar above the high pass (5kHz) filtered mean cylinder pressure, sampled at 1 Msample/sec. [3, 16, 20]. Also indicated are maximum rate of pressure rise RPR_{max} [23, 24] and maximum amplitude of cylinder pressure oscillation, DEV_{max} [25, 26]. As discussed previously, the values of these parameters vary around the cylinder, the value of KIrms at Position 1 (that generally adopted for reference) was 5.18 bar. Recent work suggests that there may be more reliable measures of knock intensity [27]; nevertheless the chosen parameters allow ready comparison with earlier studies at Leeds and elsewhere.

The initial autoignition occurred at three centres, when the estimated mean end gas temperature was 780K at 4° aTDC (Frame 26); the spark timing was 25° bTDC. The shapes of the autoignited areas suggested merging of several separate autoignition centres in the period between frames. In the subsequent frame all of the end gas (apart from a thin strip adjacent to the cylinder wall) became engulfed in flame and particle streak velocities in the burned gas region ranged from 130-200 m/s (c.f. order of 50 m/s in the previous 25 μs exposure period). The cylinder pressure rose significantly at this crank angle (5.1° aTDC). Peak cylinder pressures occurred a little later, to levels of about 100 bar; had transducer frequency response been high enough, transient excursions above this pressure would have been recorded.

MODELLING - The initial flame front position was specified triangle by triangle on the basis of the film data at the onset of autoignition and read in from a data file. Three autoignition centres were placed at positions corresponding to the middle of the principal regions of autoignition first observed on the film images. These were set to a temperature of 1000K. A reasonable fit to the experimental data was achieved with a temperature gradient (g) of –5 (62.5 K/mm) about each centre and a base end gas temperature of 750K (yielding a mean unburned gas temperature close to the 780K computed on the basis of the pressure record and flame position [3]). The complex flow patterns for this problem resulted in immediate heavy mesh refinement. Thus it proved useful to let the user refine the mesh a priori. To allow this the adaptivity module was modified to allow user specified mesh refinement around a specific location.

Runs were performed with fixed triangular meshes with 512, 2048 and 8192 (Level 3,4 and 5) elements respectively and adaptive meshing with the maximum number of triangles set to 8192.

The resultant computed pressure histories at the four monitoring positions are set out in Fig. 4. With increasing refinement, predicted pressure rises following autoignition occurred earlier. The more efficient adaptive code gave results very close to those with a fixed grid at Level 5. The evolution of the grid refinement is evident in the 2-D plots of temperature development in Fig. 5. Results with an adaptive Level 6 grid are also shown in Fig. 4; these calculations were terminated after solving to about 30μs, because of excessive run time. To that

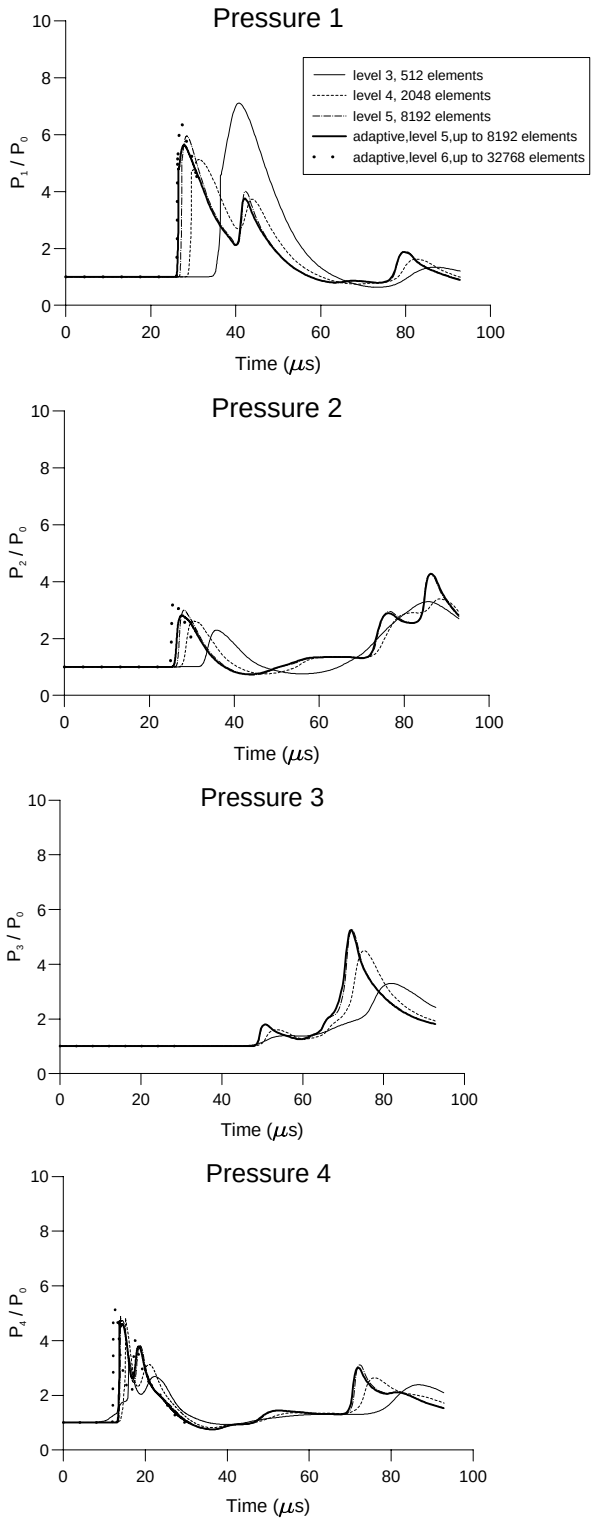

Fig. 4 Modelled pressure-time histories at four monitoring points as a function of grid refinement (engine conditions as Fig. 3)

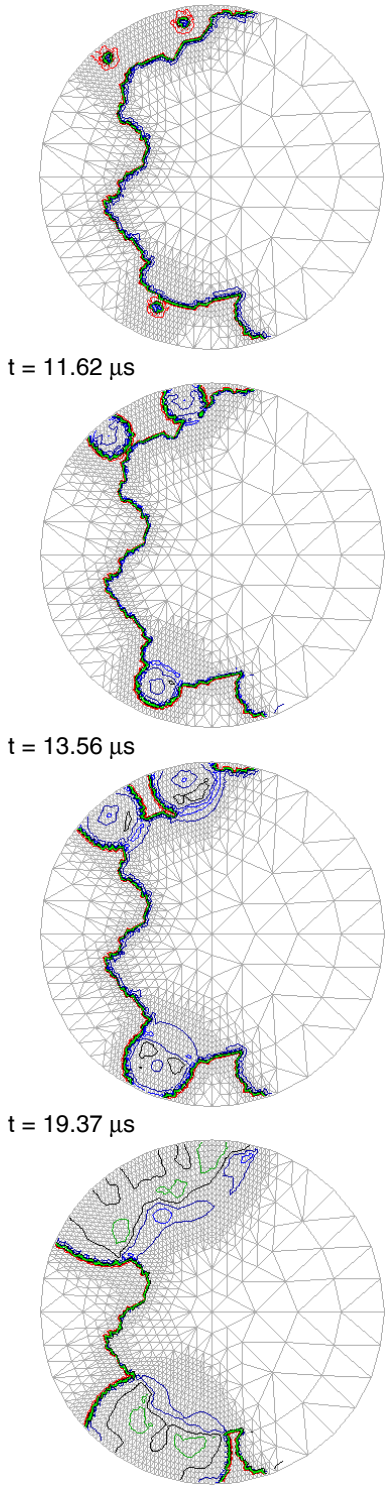

Fig. 5 Autoignition centre temperature development, showing adaptive grid refinement (Level 5 adaptive grid, autoignition centres at 1000K, temperature gradient –5)

point, results were similar, with slightly faster autoignition development to marginally higher overpressures. It is clear that even with the advanced features of SPRINT2D, a fine grid is required to simulate the autoignition development. Specialist information on other computational features and comparisons with the efficiency of the LUMAD code are available elsewhere [13, 19]. A Level 5 adaptive grid was adopted for all subsequent computations reported in this paper.

It can be seen from Fig. 5 that at first all three centres grew relatively slowly. However, between the second and third computed sequence, the two adjacent centres at the top of the diagram (11 o'clock) rapidly accelerated

towards each other, giving rise to a transient pressure spike of $5P_o$ at the nearby monitoring position, Site 4. This acceleration was likely to have resulted from interaction between the centres, as suggested previously [3]; for the merged centres and the other centre (at the bottom of the picture) then grew relatively slowly until they again accelerated and met with a large pressure excursion (to $7P_o$) at Site 1 after about 25μs. The first pressure rise noted at Site 3 (in the burned gas region, near the spark plug) occurred some 50μs later.

In comparing theoretical and experimental pressure data, the very different timescales should be noted – in the experiment 1° crank angle roughly corresponds to 100μsec. The first computed transient pressure excursion to a peak of $5P_o$ (~250 bar) occurred in a period of the order 1μsec (0.01° crank angle), rising and falling back close to the initial pressure in about 20μsec (0.2° crank angle). The pressure transducer would be incapable of recording such events; the transducer diameter was large compared to the width of strong pressure waves traversing it (resulting in spatial averaging) and its dynamic response was quite inadequate for such fast events. The transducer would have recorded some mean pressure over a timescale rather longer than that shown in Fig. 4. Nor could film and pressure record synchronisation be considered accurate to microseconds. The pressure oscillations noted in the experiment (frequency ~6kHz) took about 170μs per oscillation. Hence the successive rises in pressure noted at a point in Fig. 4 were reactions to separate events occurring in the end gas, rather than "knock" in-cylinder oscillations. After the initial fast reactions in the end gas, the pressure disturbances would settle to the classical oscillations at the natural frequency for the engine. Computations were not routinely allowed to continue long enough to show this, since it would have been exceedingly expensive in computer time and to little effect. It is argued here that the (relatively slow) "knock" pressure oscillations are merely a consequence of the mean end gas reaction rate (on the timescale of those oscillations). Although perhaps important in terms of noise, the strength of such oscillations is not necessarily a reliable indicator of the potential for material damage to the engine [8]. The latter is a function of the *mode* of end gas autoignition; it will be shown later in this paper that it is quite possible to have a potentially damaging developing detonation event at lower knock intensity (derived from pressure oscillations) than for a thermal explosion event.

Shown in Fig. 6 are computed particle tracks for a 30μs interval (similar to the experimental film exposure time) for comparison with the experimental streak plots shown in Fig. 3. To compute the particle tracks the routine previously developed [3] for LUMAD, to estimate particle velocity from local gas velocity using a drag coefficient, was incorporated into SPRINT2D. The correspondence between the experiment (Frame 27, Fig. 3) and model, Fig. 6, can be seen to be quite good. Shown in Fig. 7 is the computed lag in particle velocity relative to local gas velocity for one of the particles shown in Fig. 6. The particle velocities were of the same order as noted in the experiments, suggesting gas velocities of the order 500m/s within the burned gas region.

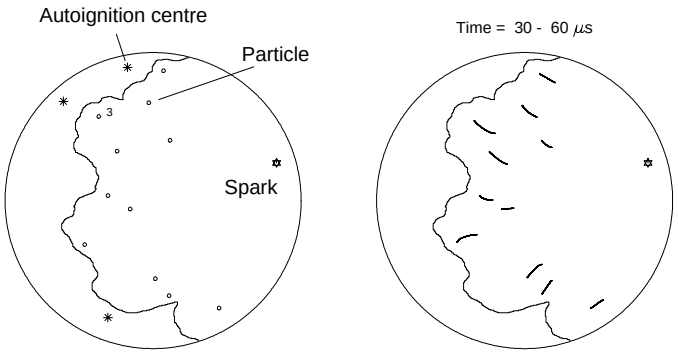

Fig. 6 Computed particle tracks (for time interval 30-60μs after centre autoignition, assumed particle diameter 40μm and density 800kg/m^3)

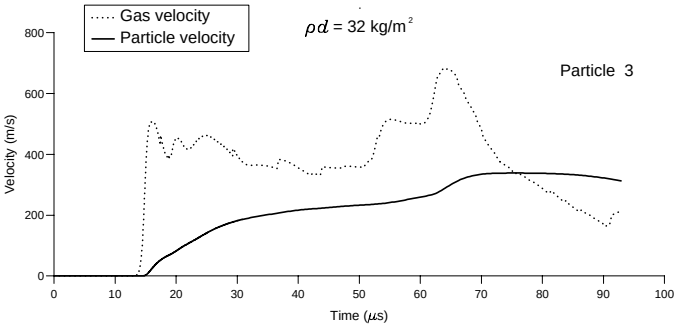

Fig. 7 Computed particle and local gas velocity for Particle 3 (c.f. Figs. 3, 6)

In filmed events, autoignition was observed in small areas (rather than points) – this might of course be related to inadequate film resolution. Nevertheless, to investigate the effect of this, computations were repeated with the point centres replaced by areas of 2mm and 4mm diameter. However, for a given temperature gradient from the centre edge, very little difference was observed in computed results. Similarly, computations were made with the linear temperature gradient replaced using a cosine function to generate an S-shaped temperature distribution between the autoignition centre and the surrounding unburned gas at the base temperature. Such a distribution was considered to be more physically realistic. Again the effect on subsequent autoignition development proved marginal, with the effect of mean temperature gradient dominant.

AUTOIGNITION CHEMISTRY MODELLING - As stated previously, in both the original LUMAD code [6, 3] and in preliminary application of the SPRINT2D program, a simple one step Arrhenius expression was adopted for the source term in the energy equation to demonstrate the various modes of end gas autoignition development.

The values of the Arrhenius parameters employed were those originally suggested by Zeldovich [16]. Later work by Bradley et al [10, 11] has demonstrated the sensitivity of the modes of autoignition to these parameters. In recent years, development of complex chemical models (and "reduced" versions of them) for representative engine fuels [28, 29] has matured to the point where they can be applied with some confidence. In the current study a 55 species and 145 reaction scheme, for iso-octane/n-heptane mixtures has been employed [14]. The scheme was derived from a somewhat more sophisticated 61 species and 263 reaction model, with both calibrated against experimental data.

AUTOIGNITION ONSET - Shown in Fig. 8 is an unburned (end gas) temperature – crank angle history for a typical moderate knock cycle with the Leeds research engine operating on a iso-octane/n-heptane fuel blend of octane rating 90. The "experimental" mean gas temperatures have been deduced from the cylinder pressure history, assuming no end gas reaction, using the thermodynamic analysis described previously [3]. The unburned gas temperature can be seen to increase progressively, in response to compression by piston motion and reaction to main flame propagation, to that crank angle (indicated by the dashed vertical line close to TDC) where end gas autoignition was first noted in the film record of this particular cycle. Thereafter the temperature (in accord with cylinder pressure) rises more rapidly to the point where the analysis was curtailed at the onset of (knock) oscillations in the pressure record. The pressure-temperature history was used in conjunction with the chemical scheme of Pitsch and Peters [14] to determine a revised unburned gas temperature allowing for reaction in the end gas, assuming pressure relaxation to the experimentally measured value at each value of crank angle [30]. The resultant "modelled" end gas temperature is also shown in Fig. 8. For this particular cycle, the "reacting" mean end gas temperature remains the same as the (assumed non-reacting) "experimental" temperature until about 3.5° bTDC. Thereafter the modelled temperature accelerates up to a mean temperature of about 1200K at the observed onset of autoigntion at some points in the end gas region. This is in accord with experimental measurements by Kalghatgi et al [31]. The mean temperature is of the order of 300K above the corresponding 'non-reacting' end gas temperature. (Since the photographs show that the autoignition is non-homogeneous, some regions of the end gas will be hotter and others cooler than 1200K). This clearly illustrates a mechanism for generating autoignition centre temperatures assumed in the SPRINT2D modelling, as well as accentuating more modest initial temperature gradients inevitably existing in the end gas region earlier in the cycle to those postulated at the onset of autoignition in the modes of autoignition codes. The chemical model was generally successful in predicting (via extremely rapid temperature rise) the observed onset of autoignition in experimental cycles.

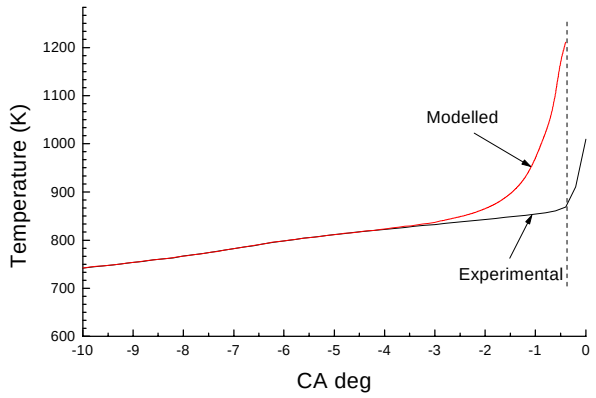

Fig. 8 End gas (autoignition) temperature development

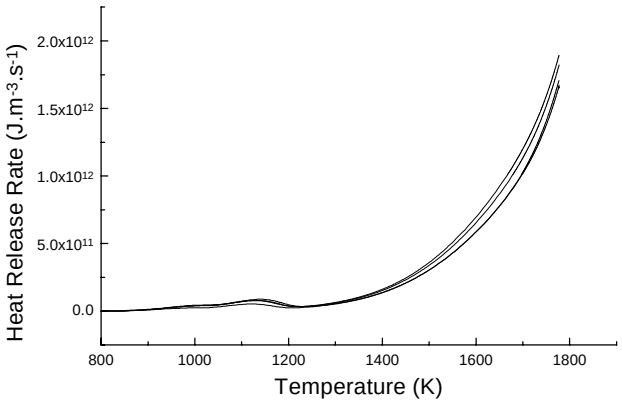

Fig. 9 Computed autoignition heat release rate – temperature profiles

HEAT RELEASE RATE - From the output of the Pitsch-Peters code, coupled to the cycle thermodynamic analysis routine, it was possible to deduce the mean end gas heat release rate. Such data are set out in Fig. 9 for a number of observed engine cycles of varying knock intensity, including that considered in Fig. 8. The heat release rate vs temperature profiles proved remarkably consistent. A seventh order polynomial fitted to an average volumetric heat release rate-temperature profile, converted to heat release rate per unit mass of fuel consumed, was subsequently used in place of the single step Arrhenius relationship in some SPRINT2D computations – as discussed later.

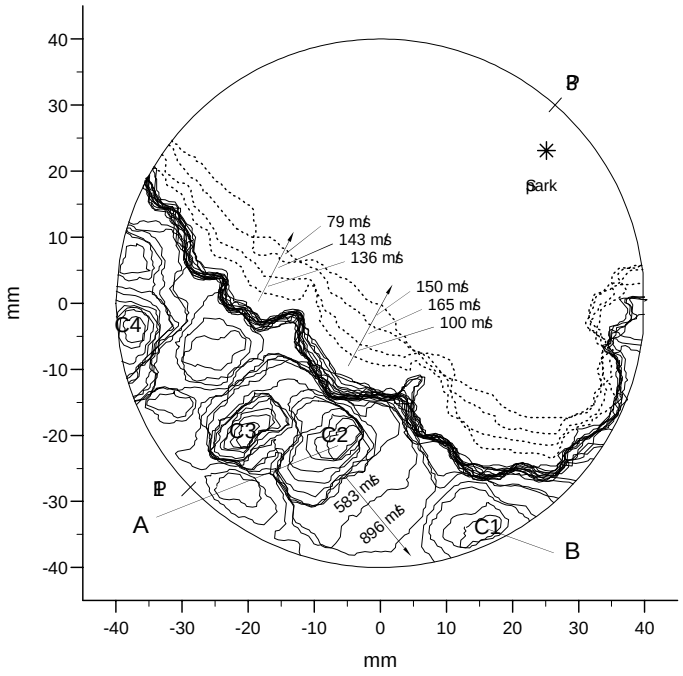

Fig. 10 Autoignition development, experimental cycle B1, moderate knock (engine speed 1000 rpm, camera speed 240,000 fps, selected frames separated by ~8μs)

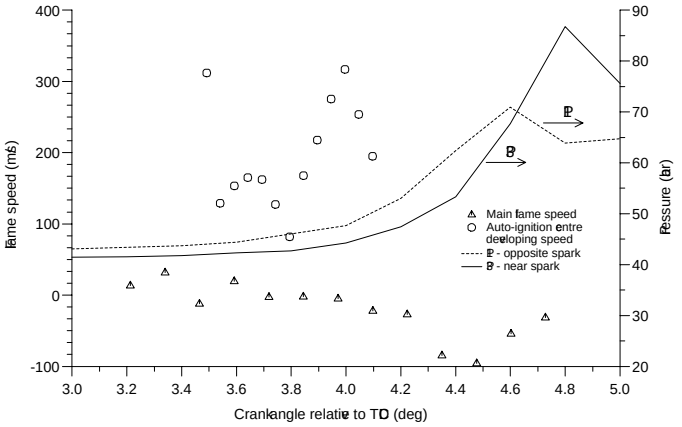

Fig. 11 Flame speed and pressure development, cycle B1

MODEL APPLICATION B

EXPERIMENTS - The speed of the camera available at Leeds was inadequate fully to track autoignition events developing at the rates suggested by the theoretical models. However, sufficiently fast schlieren images have been recorded at Daimler Benz [15], for an engine essentially identical to that used in the currently and previously [3] reported Leeds experiments, using a Cordin 330A ultra high speed rotating drum camera. The nature of the camera resulted in slightly distorted (elliptical) images, split into two halves, with a degree of irregular image rotation from frame to frame. These were corrected using image processing software developed and applied at Leeds [16] to generate the diagrams shown below.

Cycle B1 (moderate knock) - Shown in Fig. 10 are selected frames illustrating the development of end gas autoignition centres recorded at 240,000 fps (i.e. 4.21μs between frames), with the engine operating at 1000 rpm on a 90% iso-octane/10% n-heptane mixture fuel. For clarity, only every other frame has generally been traced here; i.e. intervals shown are ~8.4μs. The Leeds thermodynamic analysis routines were used to estimate the end gas temperature at the onset of autoignition (765K), as before. The knock intensity for this cycle was moderate, with KIrms = 4.4 bar; c.f. KIrms = 5.18 bar for the cycle considered previously in this paper.

The main flame front can be seen to have moved very little during the end gas autoignition events shown. This is also apparent in its mean flame speed, shown in Fig.11; this was calculated on the basis of equivalent cylindrical enflamed area [16]. Initially, the autoignition centres appear to develop relatively slowly in the "deflagrative mode". The global "flame speed" for the total autoignited area rose rapidly to a peak value of about 350m/s, just before the main flame was pushed backwards in response to end gas reaction and a significant pressure rise occurred at the transducer (P1) closest to the end gas, Fig. 11. The pressure rise was sensed later at the transducer position near the spark plug (P3). The engine at Daimler Benz was fitted with just two pressure transducers. The timing of the pressure peaks and troughs is not precise, given the relatively slow sampling rate of the shaft encoder driven data acquisition system used in this particular experiment. The "global flame speeds" underestimate the speed of localised flame propagation events within the end gas, Fig. 10. The speeds shown on this diagram were calculated from the distance traversed (between illustrated frames) along the various lines shown. Of particular interest are the very high velocities attained between the autoignition centres labelled 1 and 2 in Fig.10. A peak velocity approaching 900m/s was attained across a relatively wide front. This is possibly associated with a transition to the developing detonation mode – perhaps accompanying the creation of a more conducive temperature gradient by interaction between adjacent autoignition centres, as suggested in Ref. [3]. Nevertheless, it is interesting to note that the wall pressure rise (even close to the autoignition area) and the pushing back of the main flame occurred rather later than these events. This suggests that the main heat release rate also occurred later and was associated with the rapid burning of the highly compressed mixture between the various observed autoignition centres and (possibly) burning in the crevices induced by the strong pressure wave generated by the suggested local developing detonation [9, 15]. It is also interesting to note that the (backward) speed of the inner schlieren image of the main flame was lower than, but of the same order as, that of the particles in the slightly more severe knock cycle shown in Fig. 3.

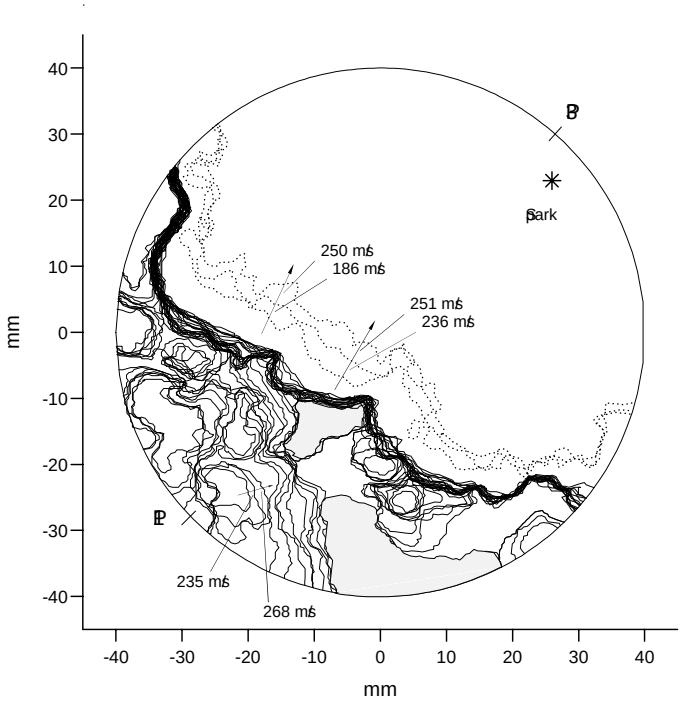

Fig. 12 Autoignition development cycle B2, severe knock (engine speed 1000 rpm, camera speed 720,000 fps, selected frames separated by ~4μs)

Cycle B2 (Severe knock) - A second film, for one of the more severe knock cycles, was similarly processed and analysed; the knock intensity for this cycle was somewhat higher, KIrms = 8.14 bar. The camera speed in this case was three times as fast (720,000 frames per second) such that the time interval between frames was only 1.42μs, although the total duration of the event filmed was correspondingly less - since only a fixed maximum length of film could be fitted in the camera. An overall picture, showing selected successive flame positions, is shown in Fig. 12. In this diagram, for clarity, tracings are generally shown only for every third frame. The entire autoignition events shown occurred in the period 0.8 – 0.44°bTDC, i.e. 60μs. Some autoignited areas were evident even in the first frame of this film; at this time the bulk of the remainder of the end gas region was characterised by the mottling effect (associated with preflame reaction) noted earlier in slower films [1]. As time elapsed the mottling effect continued and further autoignitions occurred adjacent to (but separate from) the earlier autoignition – with which they eventually merged. Later the mottling effect became much stronger in the end gas region between the autoignition centres, illustrated by the shaded areas in Fig. 12. Reaction within the mottled region strengthened (without distinct schlieren fronts) and eventually became indistinguishable from earlier autoignited areas. "Global" main flame and "mean autoignition flame speeds", calculated as before, are shown in Fig. 13. These demonstrated the same features and magnitudes as for the moderate knock cycle, although within a third of the time. As before, the pressure rises followed the autoignition events. Some local flame speeds are again shown in Fig. 12. The mean "autoignited flame speed" ranged up to 380 m/s in this case; unlike the previous cycle, no example of local developing detonation could be detected. The widespread end gas autoignition could in fact be thought to approximate quite closely to the thermal explosion mode of reaction. The main flame (as shown by the rear schlieren image) was pushed back more vigorously in this cycle – with velocities up to approximately 250 m/s, c.f. 150 m/s in the earlier case. The estimated mean end gas temperature at autoignition, which occurred rather earlier in the cycle (prior to downward piston motion), was 800K (c.f. 765K in the moderate knock cycle). It is of some interest that the knock intensity of Cycle B1, exhibiting features of the potentially damaging developing detonation mode, was actually lower than that of Cycle B2.

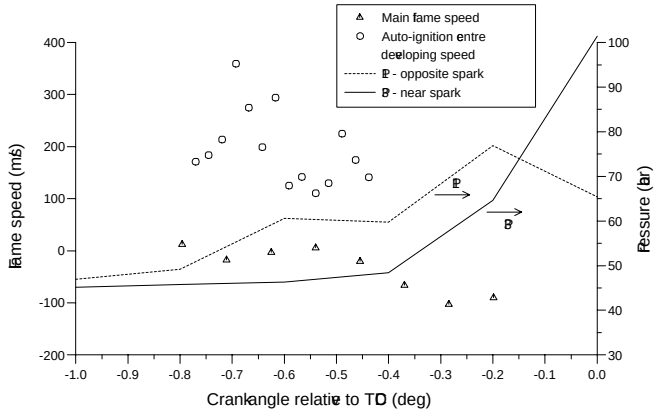

Fig. 13 Flame speed and pressure development, cycle B2

MODELLING –

Arrhenius heat release rate – The observed events for the moderate knock Cycle B1 were modelled using SPRINT2D, employing the Level 5 adaptive grid and the Arrhenius heat release rate expression. The initial conditions for the model were set close to those noted in the film/analysis, with a "base" unburned gas temperature of 765K and four autoignition centres placed close to the more significant autoignitions apparent on the photographic images, Fig. 10. The exothermic centre initial temperatures and temperature gradient were "tuned" in successive computational exercises to give a reasonable approximation to the observed events. The values adopted for the computations presented were with Centre 1 at an initial temperature of 910K, Centres 2 and 3 at 925K and Centre 4 at 915K, with a non-dimensional temperature gradient, g, of –6 (-75K/mm) assumed about each centre. The tracings shown in Fig. 14 are for successive isotherms at 2000K, taken to represent the relative positions of the "reaction front". The time increment in this diagram, in which early positions are omitted for clarity, is about 3.9μs – i.e. half that shown in the experimental case, Fig. 10.

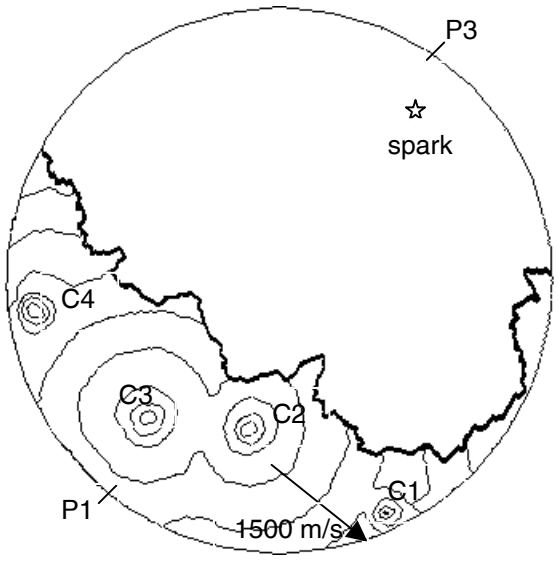

Fig. 14 SPRINT2D computations of selected successive 2000K isotherms for cycle B1 (Arrhenius reaction rate expression, isotherms separated by ~3.9μs)

The predictions showed a relatively slow initial deflagration from Centres 2 and 3, with later development of Centres 1 and 4. Centres 2 and 3 merged and connected with the main flame front after about 44μs. In the real event, several new autoignition centres developed in the region between Centres 3 and 4; additional centres were not included to simulate this in the modelled event. Between 44 and 50μs, the combined autoignition region 2/3 accelerated to engulf Centre 1 at a speed of the order 1500 m/s, suggesting transition to the developing detonation mode, albeit rather faster than noted in the experiment, Fig. 10. This was accompanied by a transient pressure of 6.5 times the initial pressure (i.e. ~325 bar) at pressure transducer Site P1, Fig. 15. This pressure excursion was predicted to last only a few microseconds. The experimentally observed pressure peak at this position was only 110 bar. However, the frequency response of the transducer used would have been totally inadequate to resolve events that fast - in practice the sampling rate of the shaft encoder driven data acquisition system used in this particular experiment was even inadequate to resolve to the frequency response of the transducer. A peak pressure of 8.34P_o (~400bar) was in fact computed for a wall position at about "6.30 o'clock". The transient pressure distribution within the end gas region, at 44.54μs, is shown very graphically in Fig. 16 – viewed from a point near transducer Site 3. It is interesting to note the high pressure spikes close to wall regions, where unburned gas movement is constrained.

Empirical heat release rate - The time elapsed from the first autoignition to complete engulfment of the end gas as observed in the film images was about 92μs; the computed events presented above took <60μs. This was considered to be associated with over-prediction of the rate of reaction given by the Arrhenius expression in the model. This is demonstrated in Fig. 17; here the rate of heat release per unit mass of fuel versus

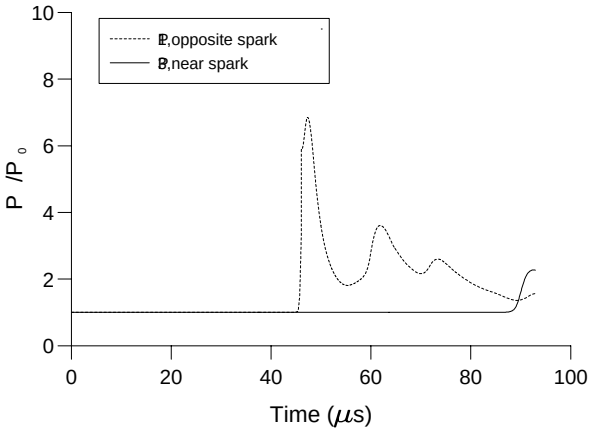

Fig. 15 Computed pressure development at "Transducer" Sites 1 and 3, cycle B1 (Arrhenius reaction rate expression)

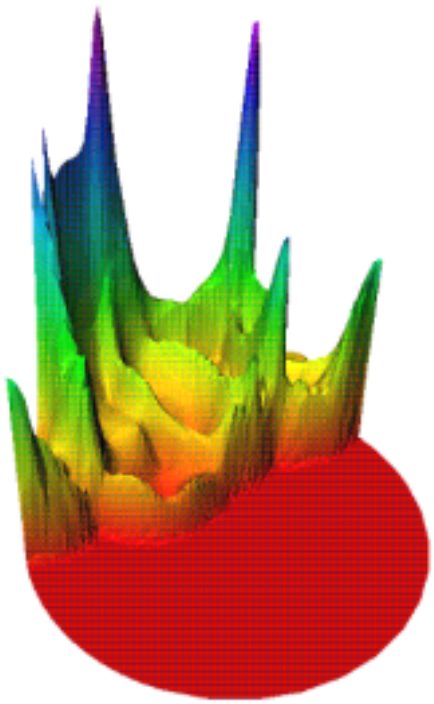

Fig. 16 Computed three dimensional transient pressure diagram at 44.54μs (viewed from position close to "Transducer" Site 3), cycle B1

temperature, computed using the Aachen chemical kinetic model coupled to an engine pressure record as described previously, is compared with that given by the Arrhenius expression. Also shown in that figure is a polynomial fit to the "Aachen" heat release rate. Although the fit at "low" temperature (relevant to the establishment of the initial autoignition centres) was not good, that to the "high" temperature" reaction (more significant in terms of subsequent development) was much better. The polynomial was adopted in place of the Arrhenius expression in SPRINT2D and the computation repeated for the same autoignition centre initial temperatures as before, Fig. 18.

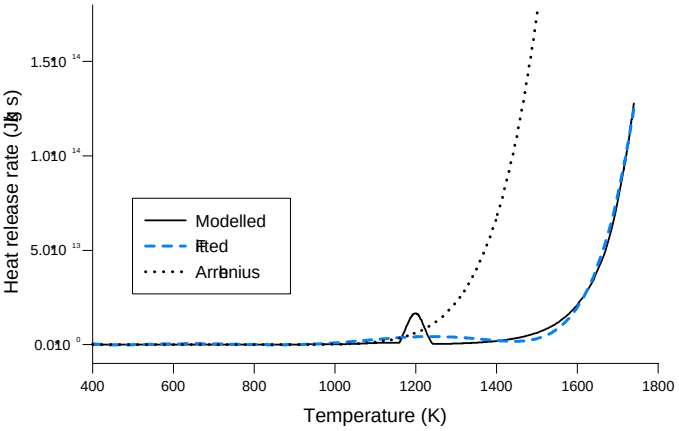

Fig. 17 Heat release rate vs temperature profile (from Arrhenius expression and chemical kinetic model fitted to engine cycle).

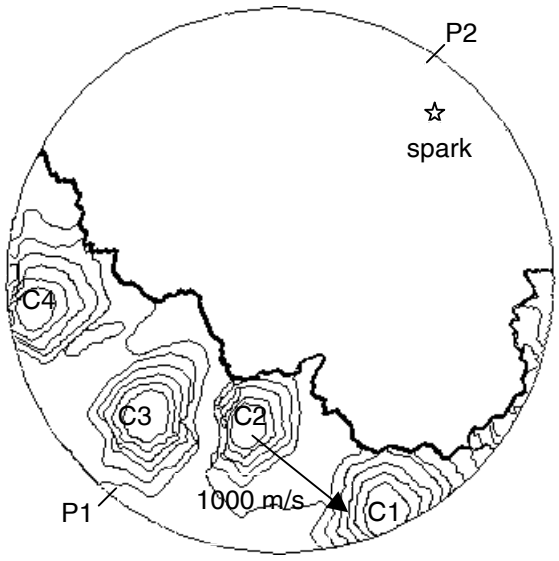

Fig. 18 SPRINT2D computations of selected 2000K isotherms for cycle B1 (with polynomial heat release rate expression replacing Arrhenius term, isotherms separated by ~8μs)

For the computations shown the linear temperature gradient was also replaced by a temperature profile given by:

$$T = T_{min} + (T_{max} - T_{min}) \cos(ax)$$

where T_{min} was set at the base temperature of 765K, T_{max} at the appropriate centre temperature; x is the distance from the centre and a is a coefficient (for these computations adjusted to give the same diameter of the elevated temperature region about the autoignition centre as with g=-6). It was reasoned that such a profile was more representative than a linear one of the small areas (rather than points) of autoignition observed on the filmed images – in practice the profile proved to have relatively little effect.

With the lower heat release rate, the overall end gas events proved slower; taking ~75μs c.f. the experimental 92μs. However the developing detonation feature between Centres 2/3 and Centre 1 was still apparent, Fig. 18. This figure, as before, shows successive positions of 2000K isotherms; the time interval in this case is approximately 8μs, similar to the experiment (Fig. 10) and twice that adopted in Fig. 14. An "apparent flame speed" for the developing detonation was now of the order 1000 m/s, closer to the 900 m/s observed in the film.

DISCUSSION

For some time it has been established that "slow" end gas autoignition events can occur with little or no knock [1, 3]; such benign post-ignition, happening with reaction rates similar to those in the main flame front, may actually be beneficial in speeding up the final stages of combustion and reducing unburned hydrocarbon/carbon monoxide emissions. There is also evidence for near simultaneous autoignition at multiple sites, approaching thermal explosion of essentially the entire end gas [1, 14, 30, 32]; such an example is shown in the current paper. Depending on the temperature and pressure (and to a lesser extent end gas mass) pertaining at the onset of a thermal explosion, this can result in mild to very severe knock intensity. With development of more sophisticated optical techniques, evidence has accumulated in support of a more violent end gas reaction involving strong pressure/shock waves [2, 4, 25], also generating moderate to severe knock. Such a cycle is also shown in this paper.

Building on the pioneering work of Oppenheim [33] and Zel'dovich et al [17], the earlier 1-D and 2-D LUMAD codes [6] gave theoretical credence for three fundamental modes of autoignition development to explain the above observations. These modes, dependent upon the local temperature gradient about the initial autoignition centre, have been termed deflagration, thermal explosion and developing detonation. Application of the more sophisticated SPRINT2D program, with its better representation of physical boundaries and improved numerical methods for handling the severe property gradients associated with strong pressure/shock waves, has shown that the earlier findings were not an artefact of the code used – even though there were significant differences in reaction rates and overpressures, computed by the two programs.

The Aachen chemical kinetic code for hydrocarbon oxidation, applied to an engine cycle pressure-time history, has shown how low temperature reaction can generate the initial temperatures assumed for autoignition centre development in the LUMAD/SPRINT2D codes. It can also explain how local temperature differences consistent with assumed local temperature gradients might be generated from initially

less marked inhomogeneities generated by imperfect mixing with residuals, wall heat transfer etc. The rates of heat release computed using the Aachen code, for the high temperature regime, proved rather less than those assumed using the Zel'dovich parameters in the original single step Arrhenius relationship adopted earlier. With the lower heat release rate incorporated (in polynomial form), SPRINT2D proved capable of reproducing the principal features observed in the ultra high speed ciné schlieren photographs of a cycle exhibiting the characteristics of developing detonation in the end gas.

Although "thermal explosion" can generate severe knock (in terms of conventional knock intensity indices), it has been shown that only the developing detonation mode is capable of generating the extreme local pressures required to provoke material damage to the piston [1, 8, 34]. Nevertheless, it was interesting to note that the knock intensity of the severe "thermal explosion-like" event exceeded that of the "developing detonation-like" event in the two ultra high speed imaged cycles presented here. This is in accord with the recent findings of Fitton and Nates [8], that knock damage does not correlate well with conventional knock intensity parameters. Standard CFD codes, with reduced autoignition chemistry for homogeneous end gas, can reproduce the lower frequency in-cylinder pressure oscillations and knock intensity parameter values noted in experiments – presumably because "global" end gas heat release rates are approximately correct. However, to demonstrate the features of more damaging developing detonation events, it is necessary to invoke end gas inhomogeneity and adopt codes such as SPRINT2D, with more sophisticated numerical procedures to cope with highly transient shock-like phenomena.

It is possible to use a model such as SPRINT2D to reproduce and explain experimentally observed events; subject to suitable choice of initial autoignition centre position, temperature and temperature gradient. However, given cycle by cycle statistical variation of the phenomena leading to these conditions (turbulent mixing, residual concentration etc.) it is impossible, in advance, to predict the mode of autoignition development and potential for material damage. With modern engines (having adaptive ignition control systems) operating at the knock threshold under certain operating conditions, it is inevitable that some cycles will experience post-ignition. It is possible that some of these autoigniting cycles may transform into "developing detonation-like" events (even at low nominal values of various knock intensity parameters). What options are therefore available to the engine designer?

(i) Adopt stronger materials, capable of withstanding transient overloading, for the piston; or cap the piston with such materials.
(ii) Adopt revised designs of piston crown edge/top land, to minimise the damaging effects of any developing detonation wave induced crevice reaction.
(iii) Selectively cool the end gas region to delay autoignition onset; however, this may create greater temperature gradients with possible adverse effects in the event of autoignition.
(iv) Enhance turbulent mixing to destroy inhomogeneity, so favouring the thermal explosion mode. This, however, may create unfavourable temperature gradients (with contrary effect) close to cooled walls. This option is unavailable for (inhomogeneous) stratified charge gasoline direct injection engines.

A more promising approach may be revised fuel formulation. There is a long history of efforts to avoid end gas autoignition (and so knock) by increasing the "autoignition delay" of fuels. There may also be scope for modifying heat release rate/temperature profile, to delay the coupling of chemical reaction and gas dynamics essential to the promotion of developing detonation [11]. Codes such as SPRINT2D, and 1-D codes with more complex chemistry [35], may prove useful in developing these improved fuels.

CONCLUSION

The SPRINT2D code is capable of reproducing most of the observed features of autoignition and knock for a variety of end gas events.

The code suggests three fundamental modes of end gas autoignition; deflagration, thermal explosion and developing detonation. Mixed modes are possible and interaction between adjacent centres can lead to transition of the deflagration mode to either or both the other two.

Of the three modes of end gas autoignition, only the developing detonation regime is capable of generating the extreme pressure needed to explain observed material damage.

The damaging developing detonation mode may sometimes occur at lower values of conventional knock intensity indices than for the thermal explosion mode.

The coupling of chemical reaction and gas dynamics, crucial for transition to developing detonation, is dependent upon the level of end gas inhomogeneity and fuel characteristics. Sophisticated codes such as SPRINT2D are necessary to simulate such effects.

Without undue restriction on compression ratio, incipient post-ignition seems inevitable at certain engine operating conditions with modern adaptive ignition systems. Hence damage can only be avoided by measures to improve charge homogeneity, to develop fuels of appropriate characteristics or possibly by adopting design changes to ameliorate the effects of strong pressure waves/shocks in promoting top-land/crevice reaction.

ACKNOWLEDGMENTS

The work received financial support from EPSRC, CEC and Shell. The authors thank Prof Peters and Dr Pitsch (ITM, RWTH, Aachen) for the use of their hydrocarbon chemistry code. They also acknowledge stimulating discussions with Profs Bradley and Griffiths (Leeds), Prof Maly and Dr König (Daimler-Benz), Dr Kalghatgi and Prof Morley (Shell), as well as all colleagues taking part in the CEC project JOUE-0028-D-(MB) (Gas/surface interactions and damaging mechanisms in knocking combustion) led by Prof Maly of Daimler-Benz. Finally, we thank Alasdair Cairns (Leeds) for help in producing diagrams.

REFERENCES

[1]. König, G. and Sheppard, C.G.W., "End-gas autoignition and knock in a spark ignition engine", SAE Paper 902135, 1990.

[2]. Spicher, U., Kröger, H. and Ganser, J., "Detection of knocking combustion using simultaneously high-speed schlieren cinematography and multi optical fibre technique", SAE Paper 912312, 1991.

[3]. Pan, J. and Sheppard, C.G.W., "A theoretical and experimental study of the modes of end-gas autoignition leading to knock in a S.I. engine", SAE Paper 942060, 1994.

[4]. Stiebels, B., Schreiber, M. and Sadat Sabak, A., "Development of a new measurement technique for the investigation of end-gas autoignition and engine knock", SAE Paper 960827, 1996.

[5]. Heywood, J.B., "Internal Combustion Engine Fundamentals", McGraw Hill, New York, 1998.

[6]. König, G., Maly, R.R., Bradley, D., Lau, A.K.C. and Sheppard, C.G.W., "Role of exothermic centres on knock initiation and knock damage", SAE Paper 902136, 1990.

[7]. Nates, R.J. and Yates, A.D.B., "Knock damage mechanisms in spark-ignition engines", SAE Paper 942064, 1994.

[8]. Fitton, J. and Nates, R.J., "Knock erosion in spark-ignition engines", SAE Paper 962102, 1996.

[9]. Maly, R., Klein, R., Peters, N. and König, G., "Theoretical and experimental investigation of knock induced surface destruction", SAE Paper 9000025, 1990.

[10]. Bradley, D., Kalghatgi, G.T., Golombok, M. and Jinku Yeo, "Heat release rates due to autoignition and their relationship to knock intensity in spark ignition engines", pp2653-2660, 26th Symp. (Int.) on Combustion, The Combustion Institute, 1996.

[11]. Bradley, D., Kalghatgi, G.T. and Golombok, M., "Fuel blend and mixture strength effects on autoignition heat release rates and knock intensity in S.I. Engines", SAE Paper 962105, 1996.

[12]. Berzins, M. and Ware, J.M., "Positive cell centred finite volume discretisation methods for hyperbolic equations on irregular meshes", Appl. Num. Maths., 16, 417-438, 1995.

[13]. Berzins, M., Pennington, S.V., Pratt, P.R. and Ware, J.M., "SPRINT2D software for convection dominated PDEs", pp 63-80, "Modern software tools in scientific computing", Eds. E. Arge, A.M. Bruaset and H.P. Langtangen, Birkhauser, 1997.

[14]. Pitsch, H. and Peters, N., "Reduced kinetic of multicomponent fuels to describe the auto-ignition, flame propagation and post-flame oxidation of gasoline and diesel fuels", Final Report, IDEA EFFECT Subprogramme FK2, CEC Project JOU2-CT92-0162, 1996.

[15]. Maly, R.R., "Gas/surface interactions and damaging mechanisms in knocking combustion", Final Report, pp 1-55, CEC JOUE-00280-D (MB), 29 October 1993.

[16]. Bradley, D., Pan, J. and Sheppard, C.G.W., "Turbulence and flow field effects", pp 57-167, "Gas/surface interactions and damaging mechanisms in knock combustion", Final Report, CEC JOUE-00280-D (MB), October 1993.

[17]. Zel'dovich, Y.B., Librovich, V.B., Makhviladze, G.M. and Sivashinsky, G.I., "Development of detonation in a non-uniformly preheated gas", Acta Astronautica, 15, 313-321, 1970.

[18]. Joe, B. "GEOMPACK – a software package for the generation of meshes using geometric algorithms", Adv. Eng. Soft., 13(5/6):325-331, 1991.

[19]. Berzins, M. and Ware, J.M. "Solving convection and convection reaction problems using the M.O.L.", Appl. Num. Math., 20:83-99, 1996.

[20]. Pan, J., "End-gas autoignition modes and spark ignition engine knock severity", PhD thesis, The University of Leeds, 1994.

[21]. Klimstra, J., "The knock severity index – a proposal for a knock classification method", SAE Paper 841335, 1984.

[22]. Chun, K.M. and Heywood, J.B., "Characterisation of knock in a spark ignition engine", SAE Paper 890156, 1989.

[23]. Lyon, D., "Knock and cyclic pressure dispersion in a spark ignition engine", pp 105-115, "Petroleum based fuels and automobile applications", IMechE, 1986.

[24]. Cuttler, D.H., and Girgis, N.S., "Photography of combustion during knocking cycles in disc and compact chambers", SAE Paper 880195, 1998.

[25]. Nakagawa, Y., Takayi, Y., Itoh, T. and Iijima, T., "Laser shadow graphic analysis of knocking in spark ignition engines", SAE Paper 845001, 1984.

[26]. Leppard, W.R., “Individual cylinder knock occurrence and intensity in multi-cylinder engines”, SAE Paper 820074, 1992.

[27]. Burgdorf, K. and Ingemar Denbratt, “Comparison of cylinder pressure based knock detection methods", SAE Paper 972932, 1997.

[28]. Cowart, J.S., Keck, J.C., Heywood, J.B., Westbrook, C.K. and Pitz, W.J., “Engine knock predictions using a fully-detailed and a reduced chemical kinetic mechanism”, pp 1055-1062, 23rd Symp. (Int.) on Comb., The Combustion Institute, 1990.

[29]. Westbrook, C.K., Pitz, W.J. and Leppard, W.R., “The autoignition chemistry of paraffinic fuels and pro-knock and anti-knock additives: A detailed kinetic study”, SAE paper 912314, 1991.

[30]. Tindall, A., “Autoignition and knock in spark ignition engines”, PhD thesis, The University of Leeds, 1997.

[31]. Kalghatgi, G.T., Snowdon, P. and McDonald, C.R., “Studies of knock in a spark ignition engine with CARS temperature measurements and using different fuels”, SAE Paper 950690, 1995.

[32]. Miller, C.D., “Roles of detonation waves and autoignition in S.I. engine knock as shown by photographs taken at 40,000 and 200,000 frames per sec.”, SAE Quarterly Transactions, 1, (1), 1947.

[33]. Oppenheim, A.K., “The knock syndrome – its cures and its victims”, SAE Paper 841339, 1994.

[34]. Lee, W. and Schaefer, H.J., “Analysis of local pressures, surface temperatures and engine damages under knocking conditions”, SAE Paper 830508, 1993.

[35]. Goyal, A.G., Warnatz, J. and Maas, U., pp 1767-1773, 23rd Symposium (Int.) on Combustion, The Combustion Institute, 1990.